Pawel Drapala
CHEM E 499 Project Fall 2003
supervised by Bruce A. Finlayson

Introduction

In the October 2002 issue of Physical Review Letters, Dieter Braun and Albert Libchaber were the first to publish research regarding the effects of temperature gradients on the migration of DNA. For the first time, the thermal diffusion constant for DNA was determined empirically. The purpose of this project is to use the software package FEMLAB® to model the DNA trapping experiment by Braun and Libchaber.

Theory

Thermophoresis, also know as Soret effect, describes the movement of a particle due to a temperature gradient. To account for the effects of temperature on the concentration and vice versa, non-equilibrium thermodynamics couples the energy equation and the diffusivity equation by the use of phenomenological coefficients (Groot, 277). The equations take on the following form:

The energy equation

$$\rho C_p u \bullet \nabla T = k\nabla^2 T + D_C \nabla^2 C \qquad (1)$$

The diffusivity equation

$$u \bullet \nabla c = D\nabla^2 c + D_T \nabla^2 T \qquad (2)$$

In addition to concentration and temperature equations, the incompressible Navier-Stokes equation is used to obtain the velocity profile of the fluid.

The Navier-Stokes equation

$$\rho u \bullet \nabla u = -\nabla p + \rho g + \mu \nabla^2 u \qquad (3)$$

The density varies in the above equation varies linearly with temperature. In addition, the $D_C\nabla^2C$ term in equation (1) is assumed to be .

A convective instability model can be idealized with two infinity long plates. The fluid is sandwiched in-between the two plates and the bottom plate is warmer then the top. Convection can only take place if the buoyancy forces overcome the viscous drag forces of the fluid (Harrison, 2). The fluid near the bottom hot plate expands, becomes less dense and rises to the top. A plot of the fluid's Nusselt number vs. Rayleigh number has showed that the onset of convection begins at a critical Rayleigh number of 1707.7 (Silverston, 157).

Article Background

The experimental apparatus of Braun and Libchaber research involved plasmid size DNA uniformly dissolved in water. An infrared laser was used to locally heat the solution. Rising the temperature in the spot by 2.3K° created a concentration deficit of 27% (Braun, 188103-1). Figure 1 below depicts the experimental setup, as well as the overall behavior of the solution.

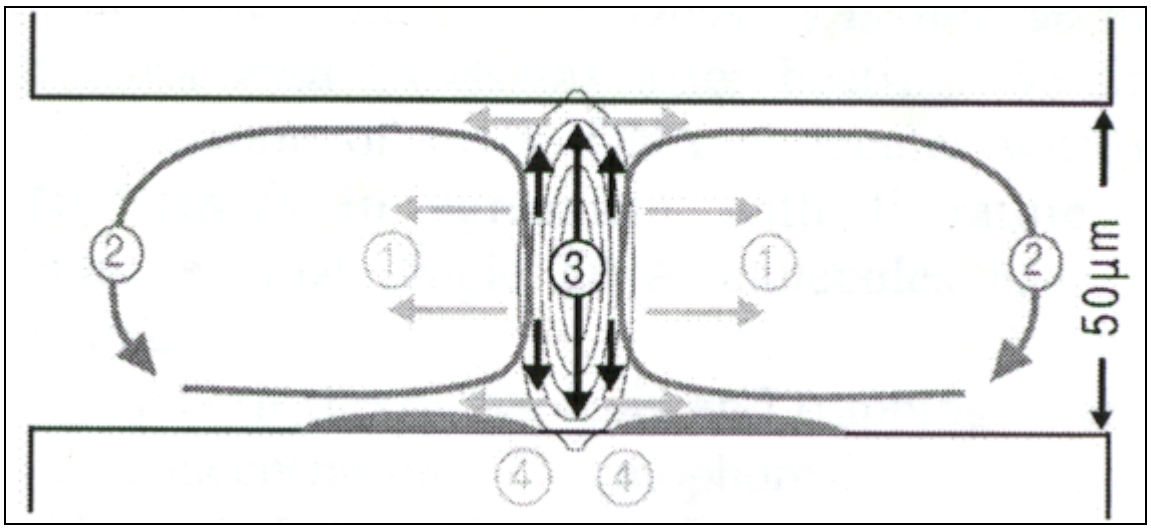

Figure 1. Apparatus of Braun and Libchaber experiment. The concentrate is repealed from the heat spot (3), caught by convection (2), and pilled on the bottom of the container (4).

An obvious perquisite of the phenomenon in figure 1 is the presence of convection. The researchers determined that the width of the container needed to be doubled from 25 μm to 50 μm in order for convection to take place.

The thermal diffusion coefficient is determined form experimental data by integrating equation (2), the energy equation, under steady state and negligible convection. The following relationship between temperature and concentration is obtained.

$$\frac{c}{c_0} = e^{-S_T(T-T_0)} \qquad (4)$$

S_T in equation (3) is defined as D_T/D, where D is the diffusion coefficient of DNA and D_T is the thermal diffusion coefficient of DNA in water. The value of D is known from literature to be $D = 3.4 \times 10^{-8}$ cm^2/s. Consequently once the value of ΔT and c/c_0 is measured, S_T and D_T can be obtained. D_T was empirically determined to be $D_T = 0.4 \times 10^{-8}$ cm^2/sK.

Methods

A solution in FEMLAB involved solving equations (1), (2) and (3) simultaneously. The most convenient way to accomplish this was to express the formulae in terms of non-dimension numbers. Three non-dimensional numbers were used with the following definitions.

$$Gr = Grashoff\ number = \frac{\rho^2 \beta_T g \Delta T L^3}{\mu^2} \qquad (5)$$

$$Pr = Prandtl\ number = \frac{C_p \mu}{k} \qquad (6)$$

$$Sc = Schmidt\ number = \frac{\nu}{D} = \frac{\mu}{\rho D} \qquad (7)$$

Application of the non-dimensional groups to the concentration, temperature, and the Navier-Stokes equations yields the following equations as they appear in FEMLAB (Harris, Appendix I).

FEMLAB's Convection and Conduction equation

$$\Pr\sqrt{Gr}\cdot u' \bullet \nabla' T' = \nabla'^2 T' \qquad (8)$$

FEMLAB's Convection and Diffusion equation

$$Sc\sqrt{Gr}\cdot u' \bullet \nabla' c' = \nabla'^2 c' + \nabla'^2 T' \qquad (9)$$

FEMLAB's Incompressible Navier-Stokes equation

$$\sqrt{Gr}\cdot u' \bullet \nabla' u' = -\nabla p' + \sqrt{Gr}\cdot g_{eff} T' + \nabla'^2 u' \qquad (10)$$

A two-dimensional FEMLAB geometry was chosen to mimic the setup depicted in Figure (1). The following figure depicts the geometry.

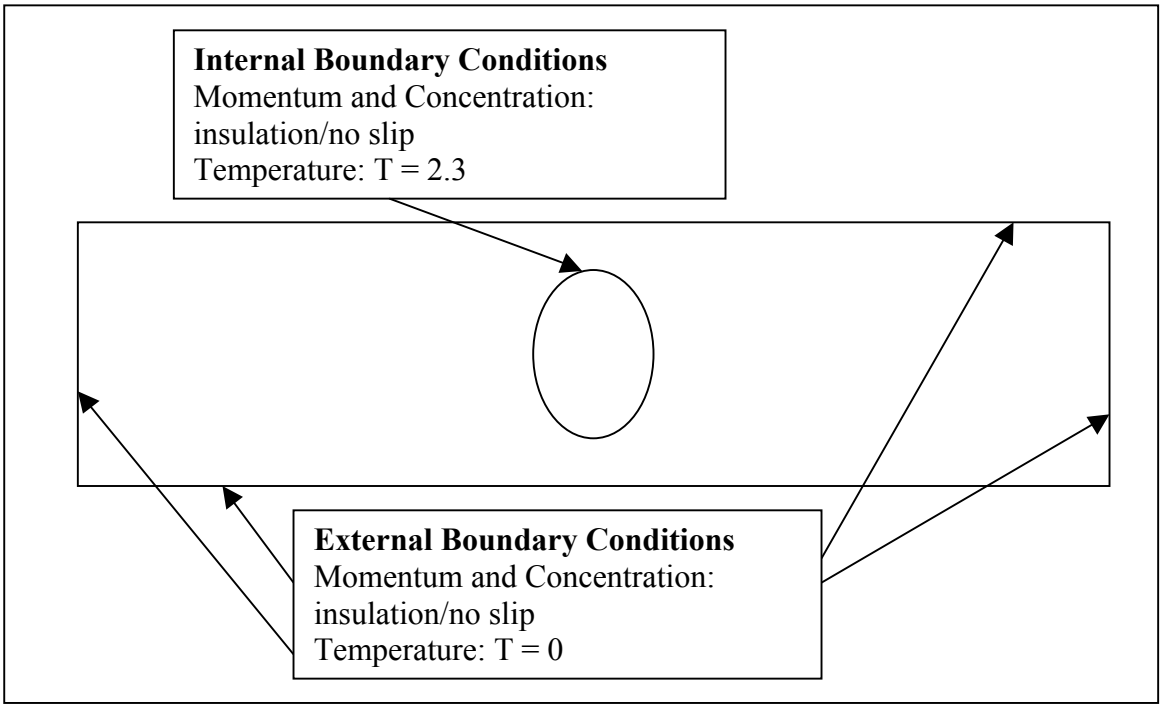

Figure 2. Boundary conditions for the specified geometry. All sides were insulated for both concentration and momentum. The temperature was set to 2.3 at the center and 0 at the edges.

The following figure depicts the geometry as it appears in FEMLAB.

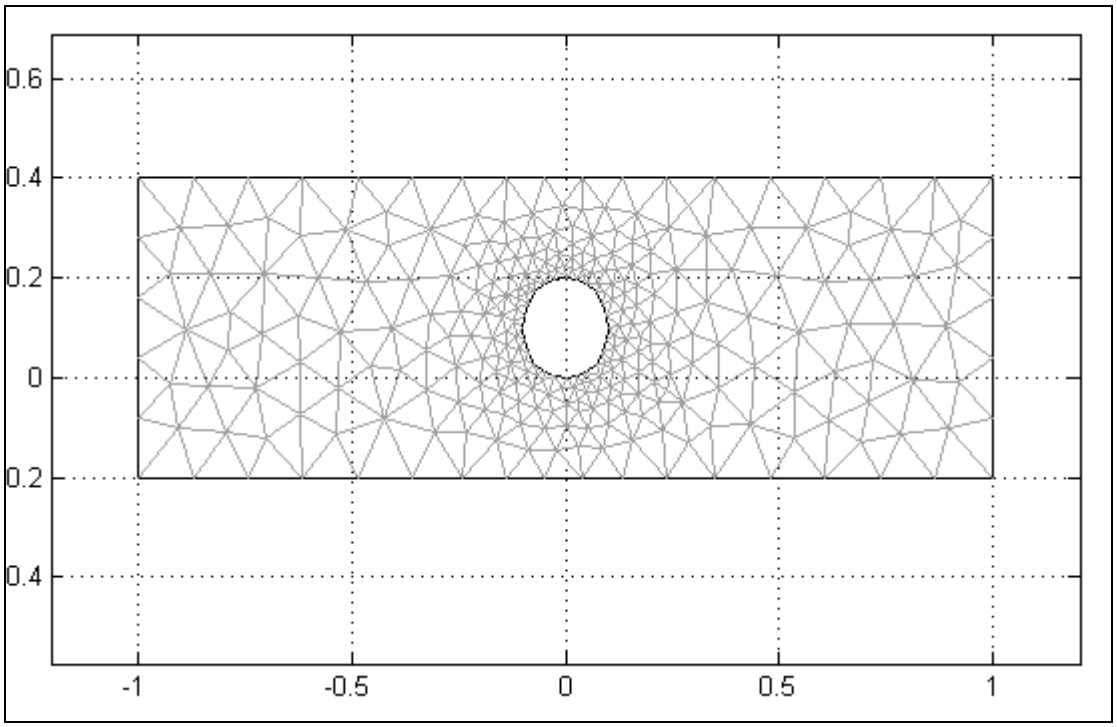

Figure 3. Designated geometry in FEMLAB's mesh mode. The mesh had 301 nodes, 68 elements, and 4845 degrees of freedom.

The specification of boundary conditions in Figures 1 and 2 is incomplete. Both the concentration and the pressure are underspecified. Consequently, without additional modification, no solution is obtained. The following procedure was taken to correct the problem of under specification. Under the point menu "view as point coefficients" was selected. Again, under the point menu "Point Settings…" was selected. The "weak' tab was selected in the resulting window. The second zero in the bottom slot was changed to "1-c" resulting in the concentration of 1 at the point. A second point was chosen, and in the same fashion a zero was changed to "-p" specifying the pressure to be 0 at the point. Figure 4 on the next page outlines the procedure.

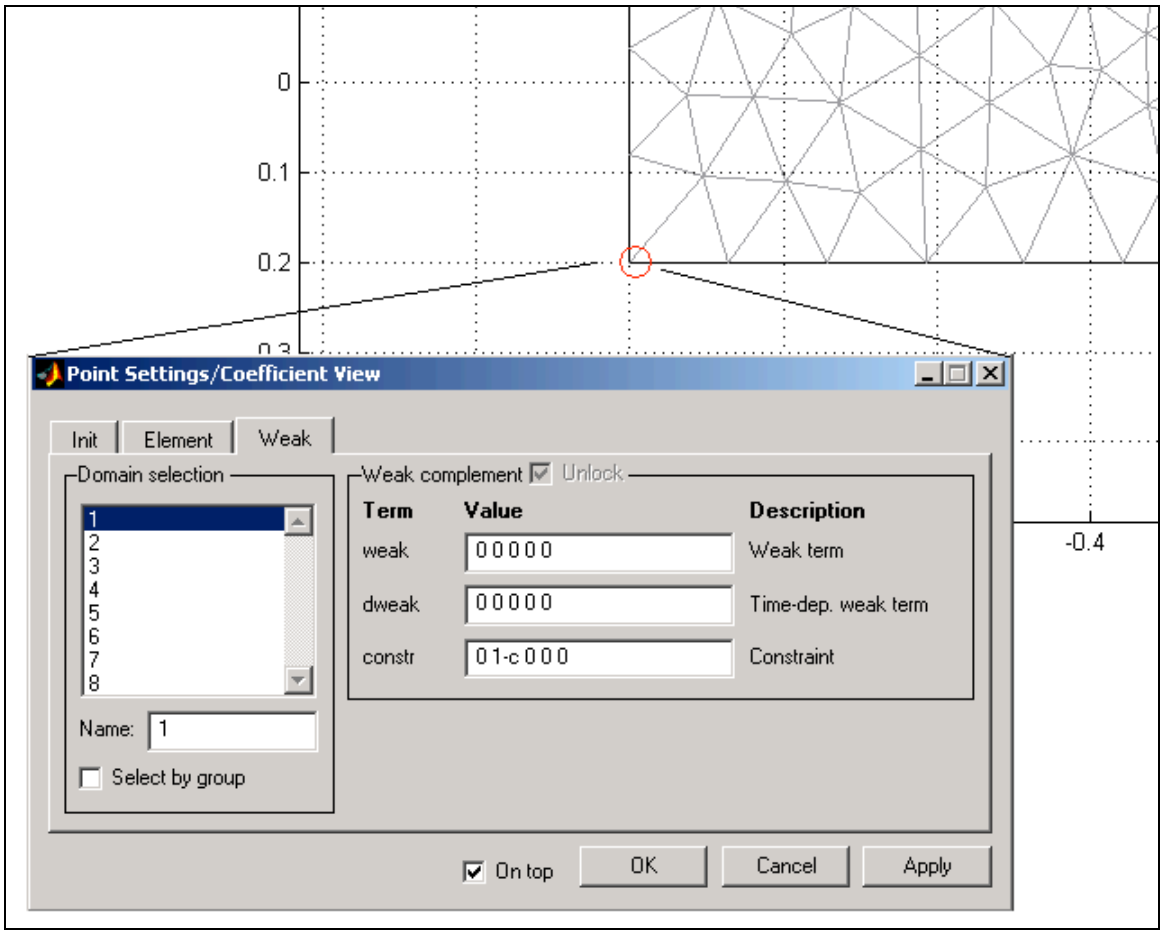

Figure 4. Changing 0 to 1-c specifies a concentration of one at the point. This procedure ensures that concentration equation converges.

Results

The following sets of figures depict the solutions obtained. Both the Prandtl and Schmidt numbers have been set to 5.3. The Grashoff number was varied from 1 to 301 by intervals of 50.

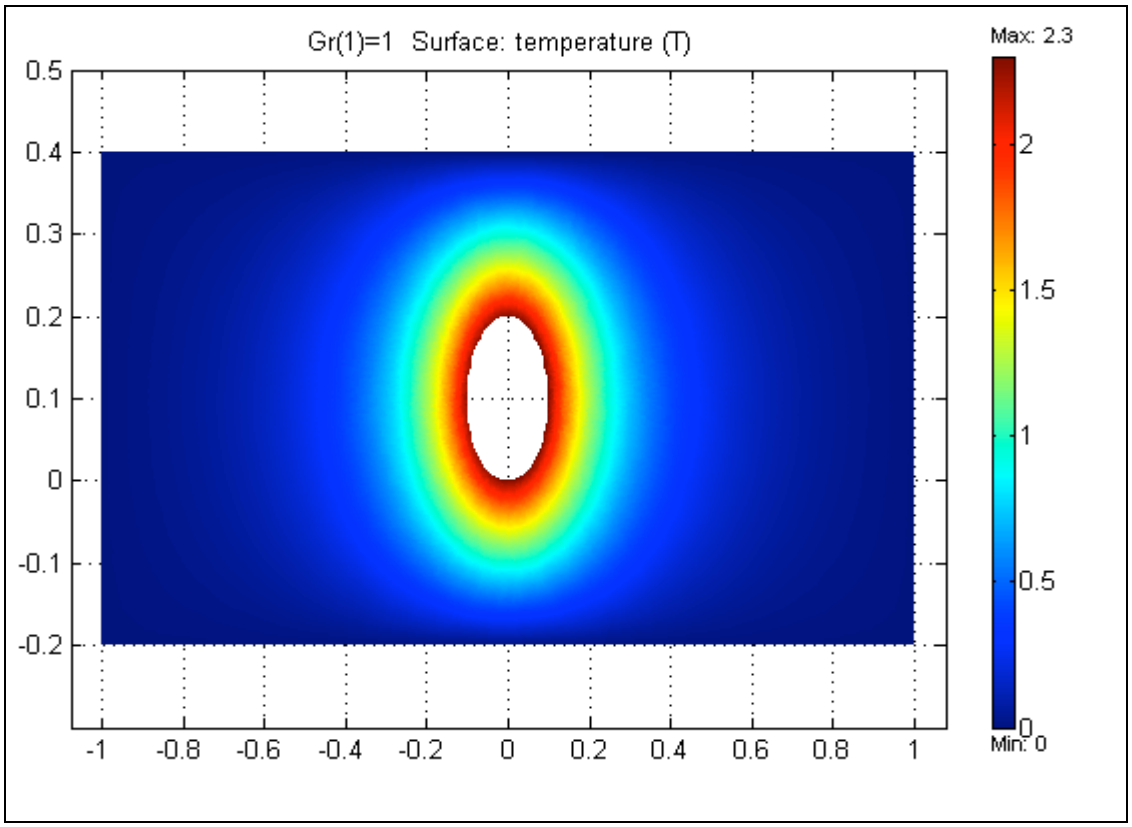

Figure 5. Solution for the temperature equation at Grashoff number of 1.

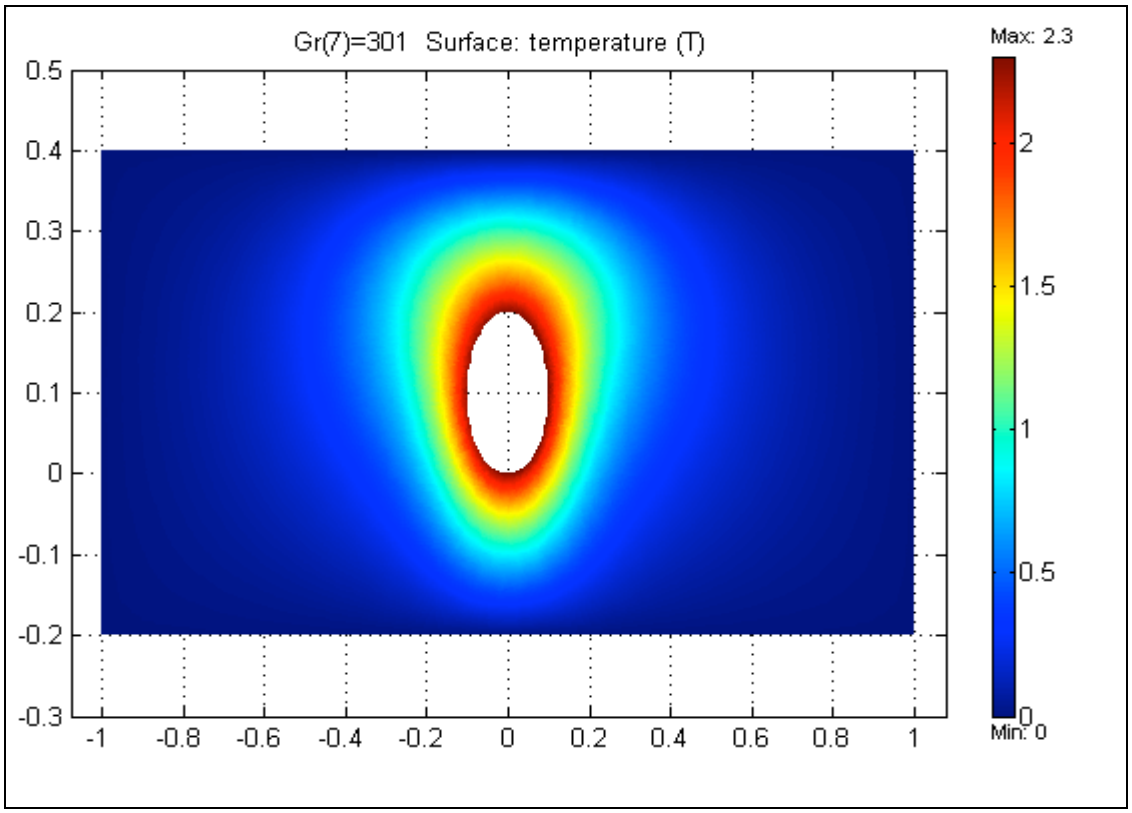

Figure 6. Solution for the temperature equation at a Grashoff number of 301.

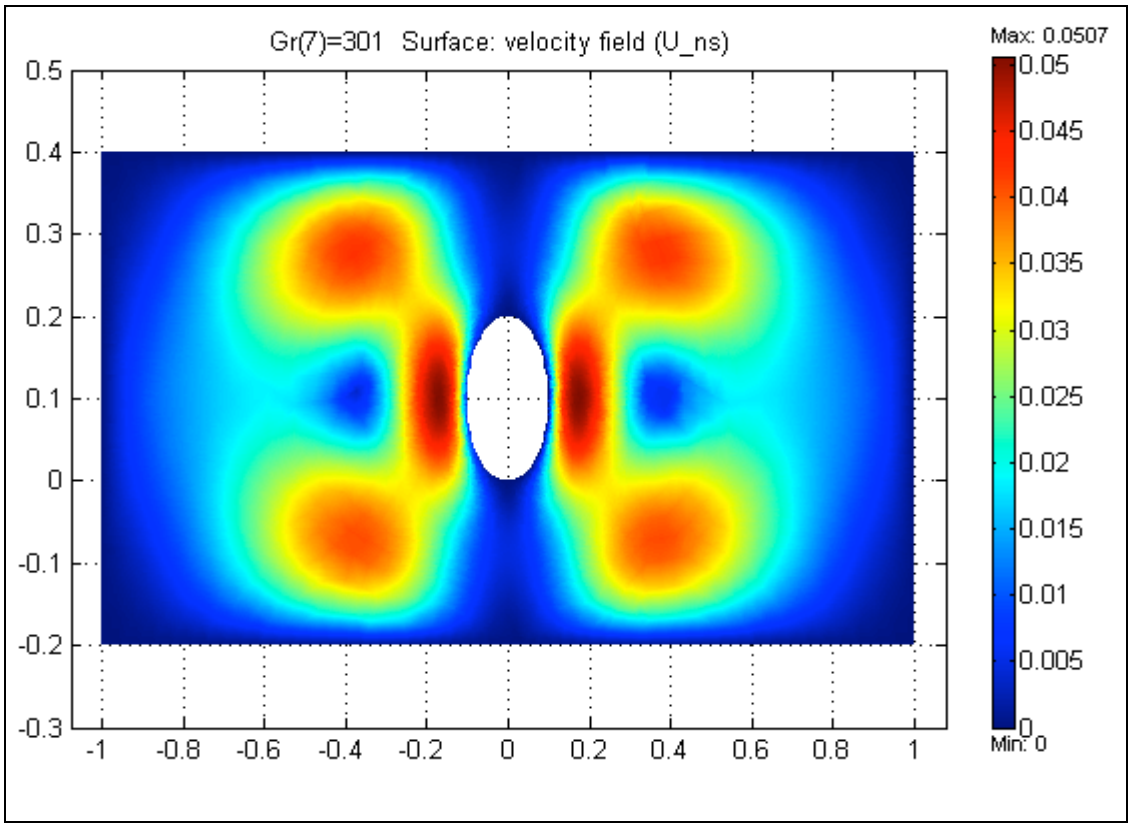

Figure 7. Solution to the Navier-Stokes equation at Grashoff number of 301.

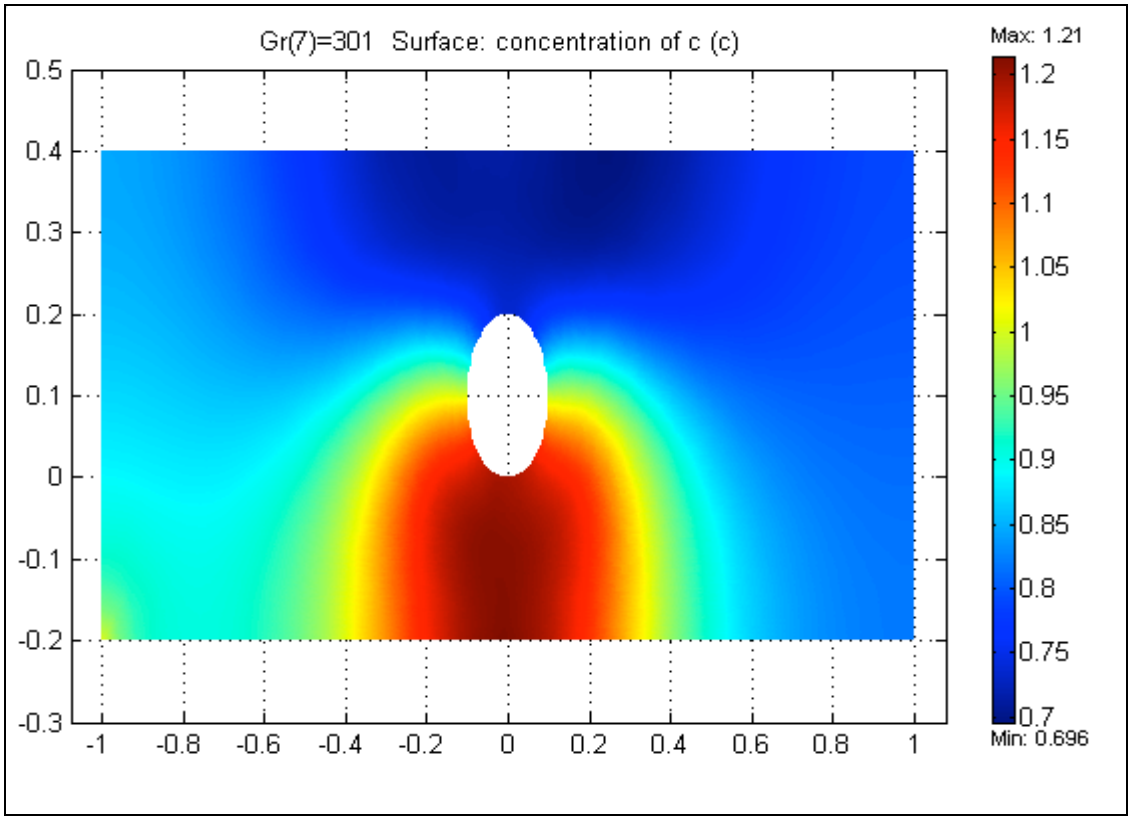

Figure 8. Solution to the concentration equation at Grashoff number of 301.

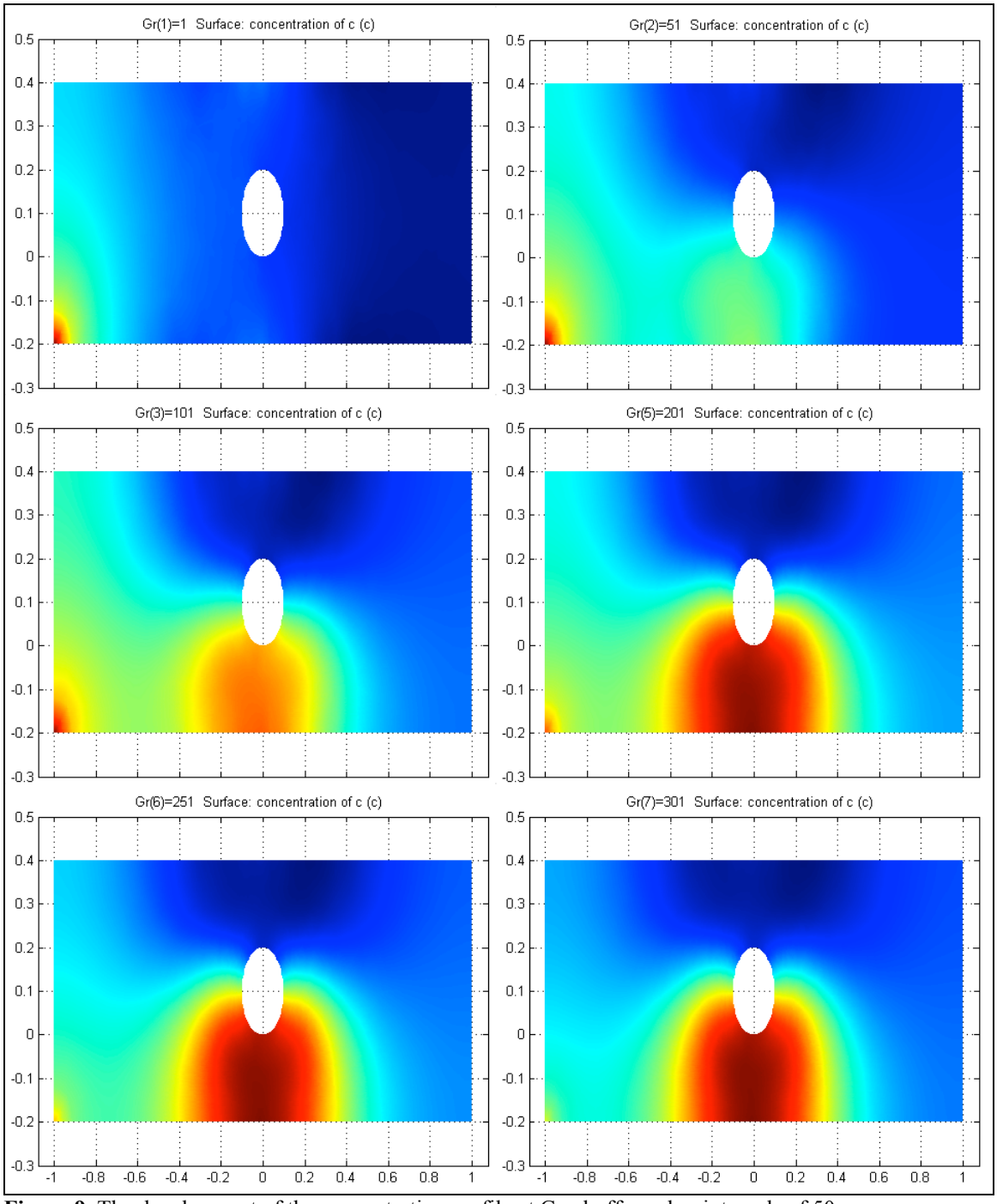

Figure 9. The development of the concentration profile at Grashoff number intervals of 50.

Discussion

The velocity profile in Figure 7 closely resembles the arrow diagram in Figure 1. The velocity exhibits a ringlike shape with maximum velocity points on left and right of the central heat spot. The maximum velocity at a Grashoff number of 301 was found to be $8.04 \cdot 10^{-7}$ m/s (Appendix). The solution of the energy equation exhibits an initial uniform profile as shown in Figure 5. At higher Grashoff numbers, the temperature profile exhibits a more oval shape due to the influence of momentum as is shown in Figure 6.

The concentration profile depicted in Figures 8 and 9 shows how the concentrate accumulates at the center of the bottom edge within the geometry. The progression towards a fully developed solution is shown in Figure 9. The appearance of the concentration profile changes very little beyond a Gr value of 301. The maximum concentration increase is 21% and the maximum concentration depletion is 30.4% at Gr = 301. This seems to be in excellent agreement with paper, where the depletion was 27%. However, unlike in the experiment, the FEMLAB model does not have a uniform depletion in the heat spot. In addition, the accumulation of contrite is at the edge of the simulation is uniform, not ringlike as in the experiment.

Braun determined that convection forces became prevalent only when he doubled the container width from 25μm to 50μm. Doubling the length in Equation 5 is the equivalent of multiplying the Grashoff number by 8. Assuming that the FEMLAB solution of Gr = 301 is equivalent to when Braun first observed convection in the experiment, a uniform concentration profile should be seen at a Gr ≈ 37. This is indeed the case, as seen in Figure 9.

The following set of plot show concentration differences at the calculated Gr numbers.

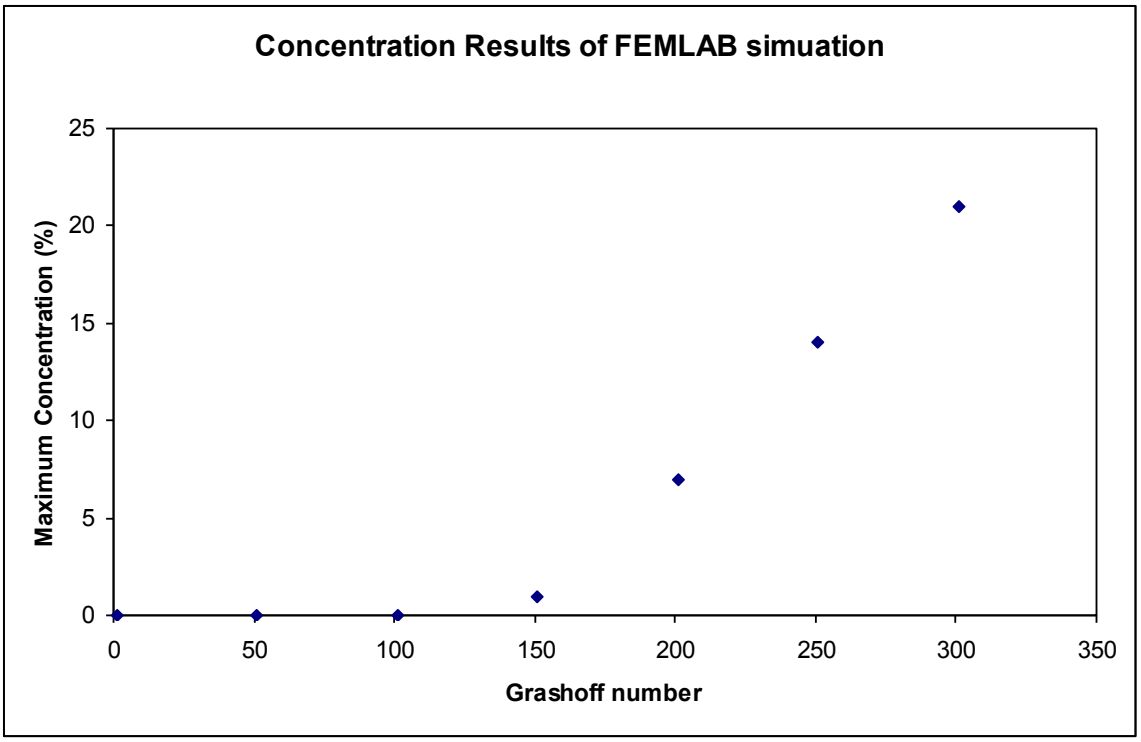

Figure 10. The maximum concentration increase of FEMLAB simulation at various Grashoff numbers.

As depicted in Figure 10, the onset of accumulation begins at a Grashoff number of 100.

Conclusion

An attempt to model the empirical result by Braun and Libchaber has met with mixed results. While both the temperature and velocity profiles seem accurate, the concentration profile does not fully resemble the experimental results.

Perhaps one of the biggest flaws of the FEMLAB simulation is that it takes place in two dimensions. A more accurate would involve setting up problem in three dimensions as shown in Figure 11 on next page.

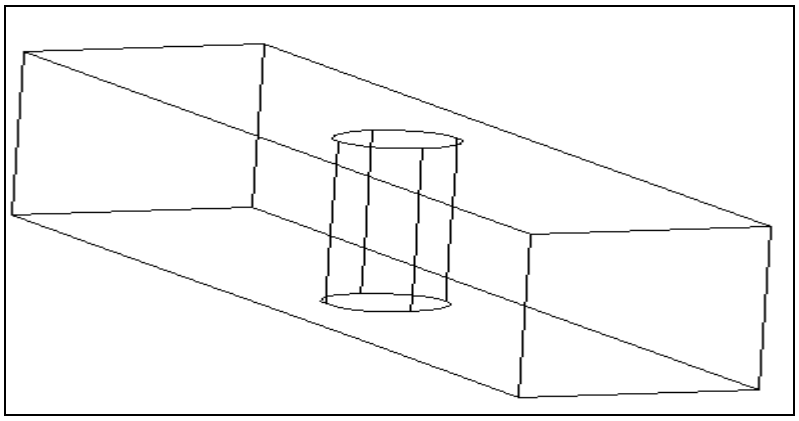

Figure 11. FEMLAB geometry as it would appear in 3-D.

However, the methodology behind this project shows that FEMLAB is capable of modeling convective instability problems. Although non-convergence is an ongoing challenge, future research into the area will involve models like one depicted in Figure 11.

Work Cited

Braun D. and A. Libchaber "Trapping of DNA by Thermophoretic Depletion and Convection." Physics Review Letters 89 (2002) 188103

DeGroot, S.R. and P. Mazur. Non-Equilibrium Thermodynamics New York: Dover Publications, 1954.

Harrison, Michael "Modeling Convective Instability in FEMLAB." CHEM E 499 project under Bruce A. Finlayson. University of Washington Chemical Engineering Department, Spring 2003.